

Steady-state multiplicity in the autohumidification polymer electrolyte membrane fuel cell

Joel F. Moxley, Sonia Tulyani, Jay B. Benziger*

Department of Chemical Engineering, Princeton University, Engineering Quadrangle A323, Princeton, NJ 08544-5263, USA

Received 10 April 2003; received in revised form 16 July 2003; accepted 22 July 2003

Abstract

“Ignition/extinction” phenomena and steady-state multiplicity were discovered in an autohumidification polymer electrolyte membrane fuel cell. At steady state, the water produced by the fuel cell reaction is balanced by water removal by the flowing reactant gas streams. Ignition, corresponding to a high fuel cell current, arises from positive feedback between the water produced by the reaction and the transport of protons in the membrane. A critical level of membrane hydration is required for ignition; insufficient membrane hydration will extinguish the fuel cell current. This new autocatalytic mechanism has an interesting analogy to the autothermal reactor.

© 2003 Elsevier Ltd. All rights reserved.

Keywords: Reaction engineering; Transient response; Multiphase reactors; Nonlinear dynamics

A glorious achievement of chemical reaction engineering was the explanation of how autocatalyticity led to ignitions and multiple steady states in the autothermal reactor. The balance between heat production by an exothermic reaction and heat removal by convective flow of the products can result in three steady states (Liljenroth, 1918; van Heerden, 1953; Uppal et al., 1974; Schmitz, 1976).

We operated a simplified polymer electrolyte membrane (PEM) fuel cell and discovered steady-state multiplicity arising from a positive feedback coupling the transport of protons with the reaction product. Extinction/ignition phenomena resulted from the balance between water produced in the fuel cell and water removed by convective flow of gases through the cell.

In this note, we briefly describe the stirred tank reactor (STR) PEM fuel cell. Experimental results of steady-state multiplicity and the dynamics of ignition for the autohumidification STR PEM fuel cell are presented. A physical model is introduced to explain how the variation of proton conduction with water activity produces autocatalysis. Detailed papers describing the differential PEM fuel cell and its application to elucidate PEM fuel cell operation (Benziger et al., (2003) submitted) and the modelling of the fuel cell dynamics (Chia et al., (2003) in preparation) are being submitted elsewhere.

The operation of the PEM fuel cell is illustrated in Fig. 1. The membrane-electrode assembly (MEA), corresponding to the central region in Fig. 1, consisted of a Nafion™ 115 PEM pressed between microporous carbon cloth electrodes with Pt nanoparticles dispersed at the membrane/electrode interfaces (Raistrick, 1989) (the electrodes were purchased from E-tek, <http://www.etek-inc.com/>). The MEA had an active area of $\sim 1.5 \text{ cm}^2$ and the volume of the gas space above the MEA was $\sim 0.2 \text{ cm}^3$ at both the anode and cathode.

The PEM is a perfluorinated polymer partially functionalized with sulfonic acid groups (Nafion™). Proton conduction requires water to ionize the sulfonic acid groups and establish percolation paths through the membrane (Gierke et al., 1982). The water uptake by the PEM, λ , and the membrane resistivity, R , are functions of the water activity, a_w , with negligible dependence on temperature (Thampan et al., 2000; Yang, 2003):

$$R = 10^7 \exp(-14(a_w)^{0.2}) \Omega \text{ cm}, \quad (1)$$

$$\lambda = 1.75 \frac{15a_w(1 - 10a_w^9 + 9a_w^{10})}{(1 - a_w)(1 + 14a_w - 15a_w^{10})} \text{ H}_2\text{O}/\text{SO}_3. \quad (2)$$

The PEM fuel cell was operated in the autohumidification mode, where the water to hydrate the PEM was supplied by the fuel cell reaction itself. Hydrogen was fed to the

* Corresponding author. Tel.: +1-609-2585416; fax: +1-609-2580211.
E-mail address: benziger@princeton.edu (J. B. Benziger).

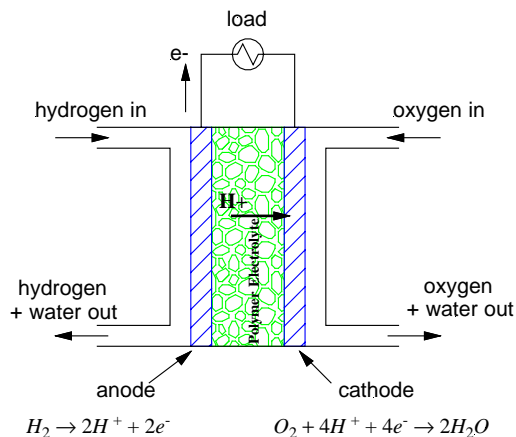


Fig. 1. Hydrogen–oxygen PEM fuel cell. Hydrogen molecules dissociatively adsorb at the anode and are oxidized to protons. Electrons travel through an external load resistance. Protons diffuse through the PEM under an electrochemical gradient to the cathode. Oxygen molecules adsorb at the cathode, are reduced by the electrons and react with the protons to produce water. The product water is absorbed into the PEM, or evaporates into the gas streams.

anode at $10 \text{ cm}^3/\text{min}$ and oxygen was fed to the cathode at $10 \text{ cm}^3/\text{min}$. The reactant residence times were greater than the diffusion times in the gas space above the electrodes to assure homogeneity of the gas compositions. The entire cell was temperature controlled and humidity sensors measured the water content in the effluent.

Membrane hydration was initialized by drying the membrane in flowing dry nitrogen ($100 \text{ cm}^3/\text{min}$) for 24 h at 60°C , followed exposure to humidified nitrogen at room temperature ($\sim 90\%$ RH at 20°C). The water uptake was determined from the integrated water lost by the gas stream as determined by its relative humidity. After hydration, the cell was heated to the desired temperature, and hydrogen and oxygen flows were initiated. The external circuit was closed through a 5Ω load resistor. The current and voltage across the load, and the relative humidity in the anode and cathode effluents were continuously recorded as the fuel cell was allowed to come to steady state. In all cases, we found 24 h was sufficient to achieve steady state.

The dynamics of the fuel cell start-up at 60°C is shown in Fig. 2. Ignition is observed above an initial membrane water content of $\lambda \sim 1.8 \text{ H}_2\text{O}/\text{SO}_3$. At lower initial water content the fuel cell current is extinguished. The relative humidity of the anode and cathode effluents both approached 0 when the fuel cell was extinguished. When $\text{H}_2\text{O}/\text{SO}_3 > 1.8$ the fuel cell “ignites” (a steady-state current density of $\sim 80 \text{ mA}/\text{cm}^2$ is sustained); the relative humidity in the anode and cathode effluents also increased to values of 40–75% when the fuel cell ignited. Table 1 summarizes steady-state currents for the ignited state from 35°C to 95°C , and the water removal rates from the anode and cathode effluents.

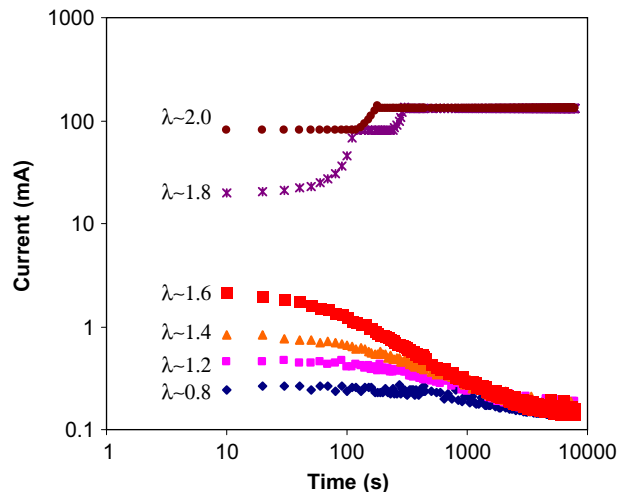


Fig. 2. Start-up of an autohumidification PEM fuel cell with different initial water contents ($\lambda = \text{H}_2\text{O}/\text{SO}_3$). The fuel cell was operated at 50°C with a 5Ω load resistance. The current through the external load resistance is shown as a function of time. The current was recorded every 10 s for a period of 6 h.

Table 1
Autohumidification PEM fuel cell performance

Temperature ($^\circ\text{C}$)	Current (mA/cm^2)*	$F_A P_w^A/RT$ ($\text{nmol}/\text{cm}^2 \text{ s}$)	$F_C P_w^C/RT$ ($\text{nmol}/\text{cm}^2 \text{ s}$)
35	78 (404)	205	200
50	80 (416)	180	215
65	78 (404)	175	220
80	76 (394)	175	200
95	72 (373)	160	200
105	31 (161)	70	90

Note: Number in parenthesis is water production in $\text{nmol}/\text{cm}^2 \text{ s}$.

A few papers have reported PEM fuel cell autohumidification operation, but those authors did not identify an ignition condition or multiple steady states (Watanabe et al., 1996; Buchi & Srinivasan, 1997). In those studies, the fuel cell was switched from a humidified feed to a dry feed, the sustained operation was observed at temperatures below 60°C . There was no measure of the water content in the membrane, nor the water content of the effluents from the cell.

Steady-state multiplicity in the autohumidification PEM fuel cell may be explained in terms of the balance of water production and water removal. The mass balance for the product (water) is given by

$$\frac{F_A^{\text{out}} P_w^A + F_C^{\text{out}} P_w^C}{\mathcal{F} RT} = 0.5 i_{H^+}. \quad (3)$$

The F 's are volume flow rates, P 's are the water partial pressures, \mathcal{F} is Faraday's constant and i_{H^+} is the current. The fuel cell current equals the effective cell voltage divided by the sum of the load resistance and membrane resistance.

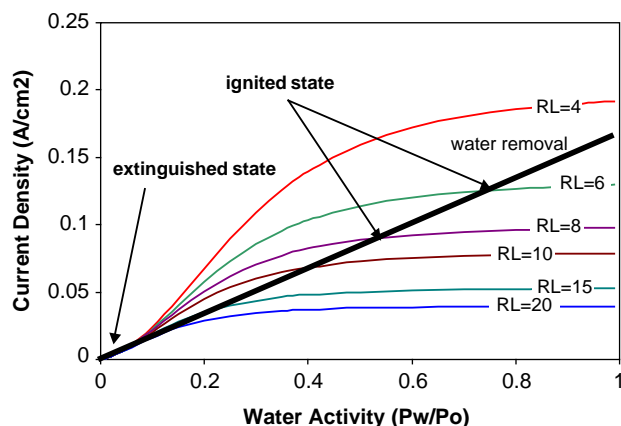


Fig. 3. Water production (fuel cell current) and water removal rates as functions of the membrane water activity for an autohumidification PEM fuel cell. The rates are expressed in terms of the current through the external load resistor. A set of curves represents the water production rates for different external load resistances. The water production is based on Eq. (4), substituting the membrane resistance as a function of membrane water activity given by Eq. (1). The water removal is based on Eq. (3). Increasing the fuel cell temperature does not affect the water removal, but increases the slope of the water removal lines.

The effective cell voltage is the thermodynamic potential (V_{oc}) reduced by the overpotential (V_{op}) associated with the oxidation/reduction reactions at the anode and cathode.

$$i_{H^+} = \frac{(V_{oc} - V_{op})}{R_{\text{membrane}} + R_{\text{load}}} = \frac{V'}{R_{\text{membrane}} + R_{\text{load}}}. \quad (4)$$

In the useful range of operation, where the activation polarization is exceeded, V' is approximately constant, with a value of 0.85 V. The membrane resistance decreases exponentially with water activity, which results in the proton current being a sigmoidal function of membrane water activity, as illustrated in Fig. 3.

Water removal and production are balanced at steady state represented by the intersections of water production and removal curves. Water removal is due to water evaporating from the membrane. Assuming the membrane is equilibrated with the gas phase, the water partial pressures at the anode and cathode are equal to water activity in the membrane times the vapour pressure of water at the cell temperature.

The water removal is a straight line in Fig. 3, whose slope increases with temperature.

Fixing the load resistance and cell temperature results in either one or three intersections of the water production and water removal curves corresponding to steady states. At a high load resistance and high temperature, there is a single low current or “extinguished” steady state. At moderate load resistances and low temperature three steady states exist. In addition to the extinguished state, there is a high current or “ignited” steady state, as well as an intermediate steady state.

Of the three steady states only two are stable. Both the ignited and extinguished steady states are stable to

fluctuations. For example, a positive fluctuation from the ignited state increases the water content in the membrane; at that condition the water removal is greater than the water generated so the system will return to steady state. The middle steady state is unstable, positive fluctuations in the water content from that steady state will cause the system to generate more water than is removed and the fuel cell will evolve towards the ignited steady state; negative fluctuations in water content from the intermediate state will drive the system towards the extinguished state. The critical water content shown in Fig. 2 corresponds to the water content of the unstable steady state in Fig. 3. According to Fig. 3, the critical water activity for ignition is 0.1. A water activity of 0.1 corresponds to a water loading $\lambda \sim 1.7 \text{ H}_2\text{O}/\text{SO}_3$, in excellent agreement with the results shown in Fig. 2.

Fig. 3 reveals that when the load resistance is low and the temperature of the fuel cell is low the ignited state would require the water activity to exceed 1, which is physically impossible. The consequences of this were observed experimentally; when the load resistance was reduced to 1.5Ω at a fuel cell temperature of 35°C the fuel cell current randomly varied between 3–4 and 120 mA/cm^2 . The water production exceeded water removal and eventually water condensed and flooded the fuel cell. The flooding inhibited mass transport of the reactant gases to the membrane/electrode interface and resulted in a drop in the fuel cell current. After a period of time, the condensed water is removed, and the current increases. This gives rise to a chaotic variation in the current over long time periods ($\sim 10^5 \text{ s}$). The simple model presented here is not adequate to fully explain this phenomenon, but gives us insight into the cause of the fluctuations.

The underlying cause of multiple steady states in the autohumidification PEM fuel cell is a positive feedback loop between the product water and the proton transport in the membrane. Increased water production increases the water content in the membrane, which decreases the membrane resistance, which in turn increases proton conductivity and the water production. The feedback loop leads to multiple steady states with ignition, extinction, hysteresis and complexity analogous to that observed in autothermal reactors. Proton conductivity in the polymer membrane increases exponentially with water content, analogous to the exponential increase in reaction rate with temperature in an autothermal reactor. Load resistance in the PEM fuel cell is analogous to reactant flow rate in the autothermal reactor. The new feature of the autocatalytic mechanism in the PEM fuel cell is the coupling between the reaction product and a transport process. This is distinct from the autothermal reactor where the reaction product is heat which accelerates the reaction rate.

We have presented the first quantitative analysis of ignition in PEM fuel cells. There are observations in the literature and anecdotal reports that the membrane must be humidified for the PEMFC to operate. But we have found no reports that attempt to predict or quantify the critical humidification level. Research on PEM fuel cells has

focused on steady-state operation and there has been little attention paid to the dynamics. Reactor models that can quantitatively model the ignition phenomena are critical for the start-up and control of PEM fuel cell systems.

References

- Benziger, J. B., Chia, E., Karnas, E., Moxley, J. F., & Kevrekidis, I. G. (2003). The Stirred tank reactor electrolyte membrane fuel cell. *A.I.Ch.E Journal*, submitted for publication.
- Buchi, F. N., & Srinivasan, S. (1997). Operating proton exchange membrane fuel cells without external humidification of the reactant gases—fundamental aspects. *Journal of the Electrochemical Society*, *144*(8), 2767–2772.
- Chia, E., Benziger J. B. & Kevrekidis, I. G. (2003). Dynamics of polymer electrolyte membrane fuel cell operation. *A.I.Ch.E Journal*, submitted for publication.
- Gierke, T. D., Munn, G. E., & Wilson, F. C. (1982). Morphology of perfluorosulfonated membrane products—wide-angle and small-angle X-ray studies. *ACS Symposium Series*, *180*, 195–216.
- Liljenroth, F. G. (1918). Starting and stability phenomena of ammonia-oxidation and similar reactions. *Chemical and Metallurgical Engineering*, *19*, 287–293.
- Raistrick, I. D. (1989). *Electrode assembly for use in a solid polymer electrolyte fuel cell*. US Patent No. 4876115, US Department of Energy.
- Schmitz, R. A. (1976). Multiplicity, stability, and sensitivity of states in chemically reacting systems—a review. *Advances in Chemistry*, *148*, 156–211.
- Thampan, T., Malhotra, S., Tang, H., & Datta, R. (2000). Modeling of conductive transport in proton-exchange membranes for fuel cells. *Journal of the Electrochemical Society*, *147*(9), 3242–3250.
- Uppal, A., Ray, W. H., & Poore, A. B. (1974). Dynamic behavior of continuous stirred tank reactors. *Chemical Engineering Science*, *29*(4), 967–985.
- van Heerden, C. (1953). Autothermic processes: properties and reactor design. *Industrial and Engineering Chemistry*, *45*(6), 1242–1247.
- Watanabe, M., Uchida, H., Seki, Y., Emori, M., Stonehart, P. (1996). Self-humidifying polymer electrolyte membranes for fuel cells. *Journal of the Electrochemical Society*, *143*(12), 3847–3852.
- Yang, C. R. (2003). *Performance of nafion/zirconium phosphate composite membranes in PEM fuel cells*. Department of Mechanical Engineering, Princeton University, Princeton, NJ.